Implementation of an Off-grid Single-phase Hybrid PV – HV Battery Inverter with Interleaved Bidirectional DC-DC Converter for Power Balancing Control in an Isolated Electrical System

Chayakarn Saeseiw[1], Piyadanai Pachanapan[1,*], Tanakorn Kaewchum[2], and Sakda Somkun[2]

ARTICLE INFO

Article history:
Received: 12 October 2022
Revised: 20 January 2023
Accepted: 15 March 2023

Keywords:
High voltage battery
Hybrid inverter
Hybrid PWM
Interleaved DC-DC converter
Off-grid operation

ABSTRACT

Two challenges for operating an isolated electricity system, such as an island or a mountain, are 1) maintaining the satisfied system frequency and voltage when the energy sources and load are rapidly changed and 2) handling the increasing harmonic distortion level from non-linear loads. This paper presents an off-grid single-phase hybrid photovoltaic (PV) and high-voltage (HV) battery inverter which can perform the fast power balancing mechanism under linear and non-linear load conditions. This hybrid inverter is comprised of a DC-AC inverter, a boost DC-DC conversion on the PV side, and a bidirectional DC-DC converter on the HV battery side. The power balance is controlled by changing and discharging the HV battery using the interleaved bidirectional DC-DC converter. In addition, the two-stage interleaved topology also benefits in reducing DC bus voltage and battery current ripples and increasing power conversion efficiency. Furthermore, the LCL filter is installed to reduce harmonic components from the DC-AC inverter outputs. Finally, the control performance of the hybrid inverter prototype is investigated in various off-grid operation scenarios. The experimental conclusions indicated that the proposed hybrid inverter efficiently managed fluctuations in PV power and load requirements as well as low and high levels of harmonic distortion.

1. INTRODUCTION

Hybrid photovoltaic (PV)-battery systems are becoming popular renewable-based energy sources for residential loads in many remote areas, such as villages, islands and hilly areas, where access to utility power is difficult [1]. As solar panel and battery costs have decreased, the hybrid PV-battery solution has sparked global interest in replacing the use of traditional diesel generator for isolated electricity systems [2]. With the assistance of battery energy storage (BES), The hybrid PV-battery system has the potential to increase energy management abilities and deliver a continuous power supply while the system is operating independently. Furthermore, the BES also supports a power balancing mechanism among PV system and local loads, as well as reducing the power fluctuation caused by PV generation uncertainly [3], [4]. Hence, the system frequency and voltage in an isolated system are improved

For small-scale isolated systems with capacities less-than 5 kW, a single-phase hybrid PV – battery system is regularly used for economic reasons. In Fig. 1, it is shown that the DC-coupled hybrid inverter is combined PV and BES with the load. which is simple and cost-effective. Besides, the hybrid inverter performs similar functions to an off-grid solar inverter but also includes an integrated battery controller inside a common unit. With the various battery technologies available today, hybrid inverters are classified by battery voltage level divided into low-voltage (LV) and high-voltage (HV) batteries. Additionally, the LV batteries basically operate at 48 V, while the HV batteries operate in between 200-500 V [5].

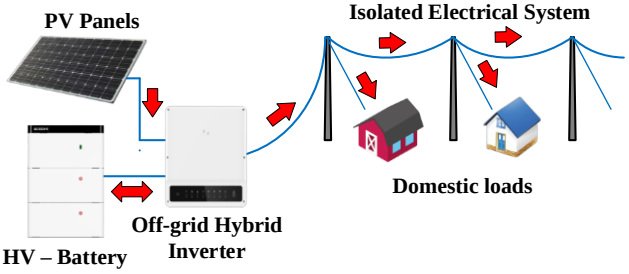

Fig. 1. Diagram of a DC-coupled hybrid PV-battery system.

[1]*Department of Electrical and Computer Engineering, Faculty of Engineering, Naresuan University, Phitsanulok, Thailand.*
[2]*School of Renewable Energy and Smart Grid Technology, Phitsanulok, Thailand, 65000, Thailand.*
**Corresponding author:* P. Pachanapan; E-mail: piyadanip@nu.ac.th.

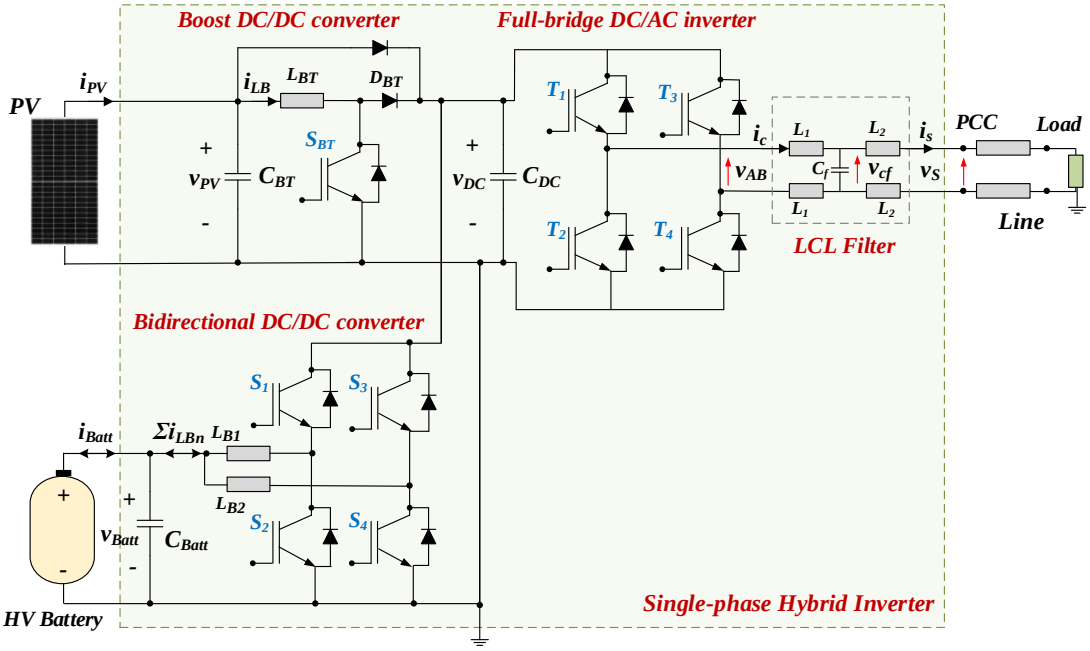

Fig. 2. The proposed single-phase hybrid inverter implemented in this work.

In the past, conventional LV batteries like lead acid were often employed as a source of energy storage due to their cost-effectiveness and simple installation. However, their weight and size are major drawbacks, necessitating a large installation space [6]. The use of LV batteries in high power applications is also limited due to their large battery current and notable loss in the voltage conversion process. Alternatively, the new generation HV batteries, such as lithium-ion, are becoming a preferred energy storage solution since their smaller size and weight, which can store more energy and provide faster charging and discharging rates than the lower one. Furthermore, as the voltage range of the PV array, which is 300 to 600 V, is extremely close to that of the voltage batteries. Temperature and cable losses of hybrid inverter is reduced, increasing the power conversion efficiency [7].

The off-grid hybrid inverter with DC coupling can convert DC power from either PV or BES to AC power via the voltage-controlled voltage source inverter (VSI). The amplitude and frequency of AC output voltage can be accomplished using pulse width modulation (PWM) control. Unipolar PWM and Bipolar PWM are two modulation techniques commonly used for open-loop voltage control of power inverters [8]. The parasitic capacitance of PV panels is the source of leakage current, which is why the hybrid PWM method has been devised to reduce it [9]. This undesirable leakage current should be mitigated to ensure safety and electromagnetic compatibility. In addition, an *LCL* filter, which has smaller filter volume and a better switching ripple reduction characteristic comparing to the simplest *L* filter, is installed to eliminate high frequency signals from the switching process [10], [11].

At the DC side, to manage the power flow for charging and discharging the HV battery system, the bidirectional DC-DC converter is employed. There are several topologies of non-isolated DC-DC converter reviewed in [12], [13]. It was found that the most promising bidirectional DC-DC converter in terms of high efficiency, current ripple cancellation, better cooling performance and high-power density is an interleaved topology. The lower current ripple requires the smaller size of filter capacitance when compared to the conventional topology, resulting in a faster control response. Also, the two-phase half-bridge interleaved topology is the most common choice for exchanging power between energy storage and DC bus [14], [15]. More than that, the interleaved bidirectional DC-DC converter is also widely applied for HV battery in electric vehicle applications [16].

In cases of residential-scale PV systems (3-5 kW), a higher voltage (i.e., 300 V – 600 V) boost DC-DC converter with the maximum power point tracking (MPPT) algorithm is typically used to extract the greatest amount of power from the PV panels. Several boost DC-DC converter topologies for PV systems were review in [17], [18]. Additionally, the popular MPPT techniques such as perturbation and observation and incremental conductance methods [19] can be applied to operate fixed PV panels at the maximum power point under various solar irradiance conditions. Moreover, the power limiting control may be included to curtail the active power produced through a PV system so as to improve system stability and voltage regulation [20].

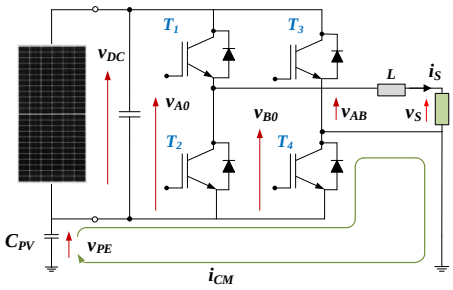

(a) Full-bridge DC-AC inverter

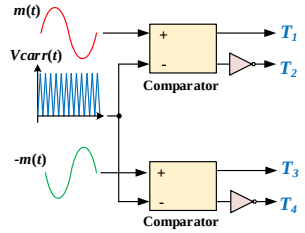

(b) Hybrid PWM

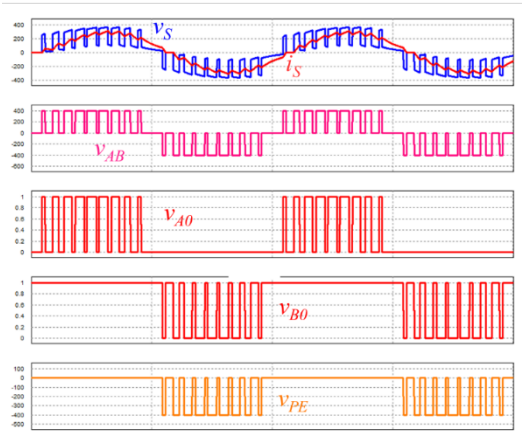

(c) PWM and output waveforms

Fig. 3. Full-bridge DC-AC inverter with hybrid PWM control strategy.

Contribution: This paper implements the hardware prototype of an off-grid single-phase DC-coupled hybrid PV - HV battery inverter that can provide a fast power balancing mechanism in an isolated electrical system under highly non-linear load conditions. Furthermore, the HV battery controller, which relies on a bidirectional interleaved DC-DC converter, is an important component in the power balancing operation by absorbing excess power from the PV system or injecting it into the load. The DC-AC inverter with an *LCL* filter and an open-loop voltage control based on hybrid PWM are used to generate an AC voltage output with lower harmonic components and leakage current from parasitic capacitance. Finally, the control performance of the proposed hybrid PV – HV battery inverter is investigated in various scenarios, including sudden load change, ramp-up, and ramp-down PV generation.

2. OFF-GRID SINGLE-PHASE HYBRID INVERTER

Figure 2 shows the implementation of the DC-coupled hybrid inverter used in this research, which consists of two DC-DC converters connected by the DC-link connection to a full-bridge DC-AC inverter. The interleaved bidirectional DC-DC converter is linked to an HV battery for energy storage management, while the typical boost DC-DC converter with MPPT algorithm is utilized to obtain as much power as possible from the PV arrays. Moreover, the *LCL* filter is chosen to mitigate the harmonic distortions from the high-frequency switching process.

During daylight hours, the dc-coupled hybrid system can continuously send power to the loads from either PV array or BES. If the quantity of electricity created through the PV system is higher than the amount of power needed by the load, the surplus power will be used to charge the battery. In contrast, when the energy produced by the PV is insufficient, the battery operates to supply additional power to the load. When the battery runs out, the DC-AC inverter shuts down, leaving the connected loads unsupplied and resulting in an interruption. Then, the battery voltage proceeds to increase when power directly from the PV system is sent straight to the BES. Once fully charged, the DC-AC inverter can turn back on and supply power to the local loads again.

Full-bridge DC-AC inverter

The single-phase VSI with an H-bridge structure is typically used to convert DC power to AC power, as shown in Fig. 3 (a). This type of inverter consists of four switches which mostly made of insulated-gate bipolar transistors (IGBTs). The PWM method is widely used for controlling frequency and amplitude of an AC signal's output voltage. In addition, the high switching frequency (kHz range) and the passive filter, *L* or *LCL*, can make the waveform of output voltage nearly sinusoidal. If the off-grid hybrid inverter is used as a stand-alone system without any other grid-forming energy sources, the open-loop voltage control, which is simple and robust, could be effective enough to allow the full-bridge DC-AC inverter to supply the power at the domestic level (< 5 kW).

When PV panels are installed, they always exhibit capacitance between PV panels and the ground towards their environment, known as “parasitic” capacitance, C_{PV}. If the inverter is a non-isolated type, the leakage current or common-mode current, i_{CM}, is introduced which can become a shock hazard. This leakage current may trip the residual-current device, causing the inverter to disconnect from the load temporarily. For a 5-kW system, the value of C_{PV} is 330-500 *nF* in the case of monocrystalline and polycrystalline modules [21].

To mitigate the i_{CM}, the hybrid PWM is selected instead of conventional bipolar and unipolar PWM methods. Fig. 3

(b) and (c) shows the hybrid PWM method and output waveforms of the DC-AC inverter. It was discovered that the switching frequency of the hybrid PWM is roughly half that of the unipolar PWM, making the switching loss is decreased. Also, the unfiltered output voltage, $v_{AB,}$ is similar to that of unipolar PWM method, whereas the common mode voltage, v_{PE}, is improved, resulting in less leakage current. However, the output current ripple generated by the hybrid PMW method is greater than that created by the unipolar PWM method. As a result, the larger size of filter is required.

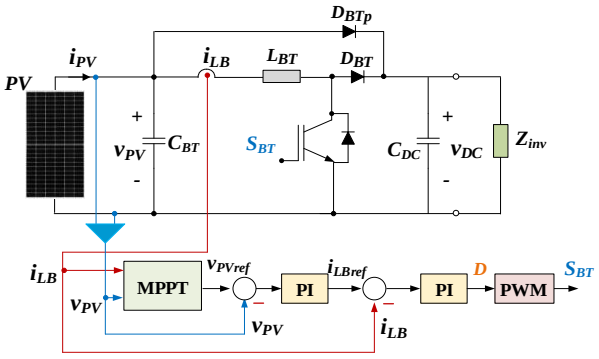

Fig. 4. The boost DC-DC converter control construction

MPPT boost DC-DC converter

The PV-side DC-DC converter operates in boost mode, focusing on obtaining the maximal power as practicable from solar irradiation. The PWM controlled boost DC-DC converter with the MPPT algorithm is shown in Fig. 4. As in the steady state condition, the inductance current, i_{LBT} is equal the PV output current, i_{PV}. Therefore, the maximum power point is tracked by measuring PV output voltage, v_{PV}, and i_{LBT}. The algorithm for the MPPT defines the voltage and current references, v_{PVref} and i_{LBref} that can extract the highest power. The v_{PV} and i_{LBT} are regulated using PI controllers, resulting in a change in duty ratio, D, of PMW signal.

The MPPT controller is only activated when the v_{PVref} is less than the reference DC bus voltage, v_{DCref}. If the v_{PVref} exceeds the v_{DCref}, the IGBT switch is turned off and the i_{PV} flows directly to the DC-AC inverter, via the bypass diode, D_{BTp}. In the case of a two-string PV system, two exactly alike boost DC-DC converters with independent MPPT controllers are employed.

Interleaved bidirectional DC-DC converter

The interleaved bidirectional DC-DC converter with a two-phase topology is implemented for charging and discharging the HV battery. From Fig. 2, the two-phase interleaved DC-DC converter consists of four switches made of IGBTs, and filter capacitor, C_B. Inductors L_{B1} and L_{B2} are used to store and release the energy during the switching operation. If PV power exceeds the load demand, the energy from PV arrays can be used to charge the HV battery through this DC-DC converter which works in the buck mode. Whereas, it runs in boost mode to discharge power from the HV battery to the load if the PV power is relatively low. The switching signals are generated using PWM method.

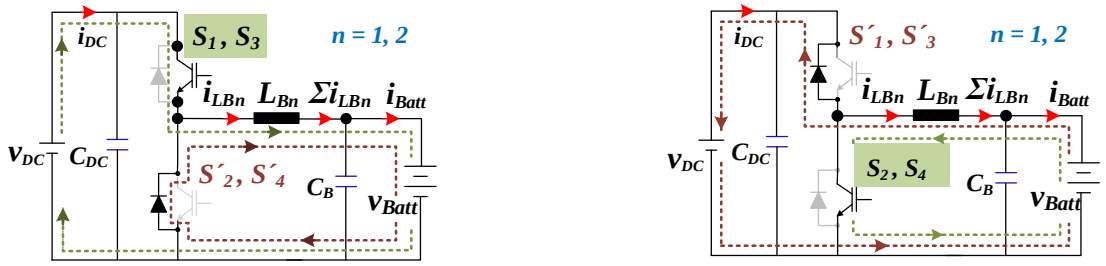

(a) Charging mode (b) Discharging mode

Fig. 5. Charging mode and discharging mode of interleaved bidirectional DC-DC converter.

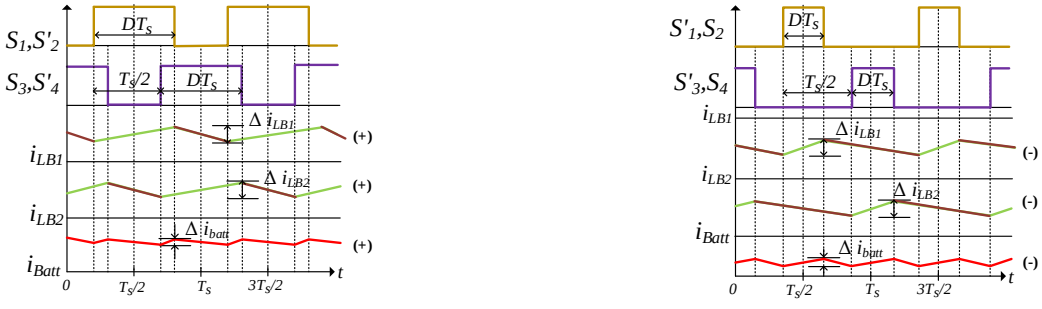

(a) Charging mode (b) Discharging mode

Fig. 6. Current waveforms of interleaved bidirectional DC-DC converter.

In charging mode, switches S_1 and S_3 are controlled while switches S_2 and S_4 are switched off. The flow of currents in the charging mode operation is shown in Fig. 5(a). Since the DC bus voltage is relatively close to the battery voltage, the switching operation is carried out with duty ratio, D, set in the range of $0.5 < D \leq 1.0$ and working in the continuous conduction mode. The switching signals for S_1 and S_3 are identical but shifted by 180° in a two-phase interleaved design. Fig. 6 (a) depicts the battery current, i_{Batt}, which is a combination of the two inductor currents I_{LB1} and I_{LB2}. It can be seen that the two-phase interleaved topology can lower the battery current ripple.

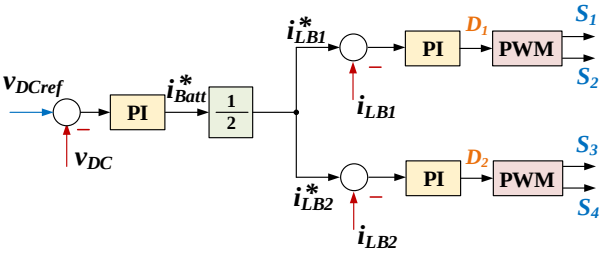

Fig. 7. The interleaved bidirectional DC-DC converter control block diagram for off-grid operation.

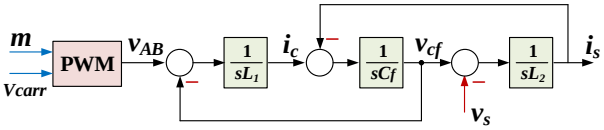

Fig. 8. The single-phase VSI with LCL filter control block diagram.

In discharging mode, on the other hand, the switching signals are sent to trigger switches S_2 and S_4, whereas switches S_1 and S_3 are not activated. The duty ratio of switching signals is between $0 \leq D \leq 0.5$. The flow of currents in the discharging mode, as well as the current waveforms are demonstrated in Fig. 5 (b) and Fig 6 (b), respectively. It is found that the flow of i_{Batt} is in the opposite direction when compared to the charging mode.

The control of interleaved bidirectional DC-DC converter for off-grid operation is shown in Fig. 7. The closed-loop control structure is composed of the following two loops: The average inductor current controller (loop of inside control) and the DC voltage controller (the outer control loop). The voltage loop regulator differentiates the reference voltage, v_{DCref}, with the v_{DC}. The voltage error is cancelled out by the PI controller and produces the battery current reference, i^*_{Batt}, for the current control loop.

In the case of two-phase interleaved circuit, i^*_{Batt} is divided in half ($i^*_{Batt}/2$) and transmitted to the current control loop. These divided currents i^*_{LB1} and i^*_{LB2} are the reference inductor currents in parallel circuits, regulating i_{LB1} and i_{LB2}. PI controllers are used to eliminating the current errors. The output of the current control loop is the duty ratio of PWM signals sent to control switches S_1 and S_3 or switches S_2 and S_4.

LCL filter

The *LCL* filter is used to minimize output current switching ripple, which is the downside of implementing hybrid PWM. Compared to the *L* filter, the *LCL* filter requires lower reactive power and has better harmonic attenuation. From Fig. 2, The *LCL* filter has three elements: an inductor on the converter side, L_1, filter capacity, C_f and an inductor on the grid side, L_2. The *LCL* filter state equations are as follows:

$$L_1 \frac{di_c(t)}{dt} = v_{AB}(t) - v_{cf}(t) \quad (1)$$

$$C_f \frac{dv_{cf}(t)}{dt} = i_c(t) - i_s(t) \quad (2)$$

$$L_2 \frac{di_s(t)}{dt} = v_{cf}(t) - v_s(t) \quad (3)$$

From (1) to (3), the block diagram of the single-phase VSI with the *LCL* filter can be drawn as Fig. 8. Moreover, the current ripple attenuation, *A*, is derive by.

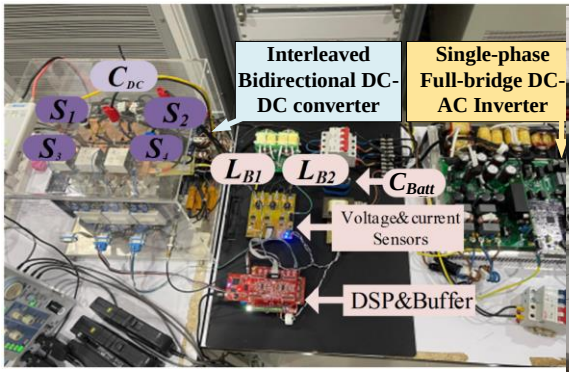

(a) Hardware prototype

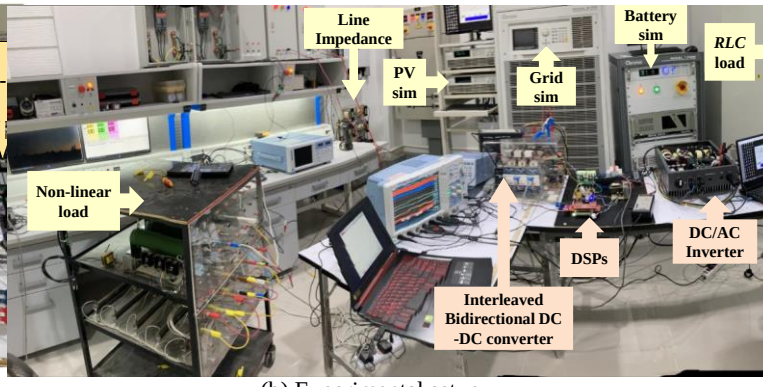

(b) Experimental setup

Fig. 9. Hardware prototype and experimental setup.

$$\frac{i_s(s)}{v_{AB}(s)} = \frac{1}{s^3 L_1 L_2 C_f + s(L_1 + L_2)} \quad (4)$$

$$\frac{i_c(s)}{v_{AB}(s)} = \frac{s^2 L_2 C_f + 1}{s^3 L_1 L_2 C_f + s(L_1 + L_2)} \quad (5)$$

$$A = \frac{i_s(s)}{i_c(s)} = \frac{1}{s^2 L_2 C_f + 1} \quad (6)$$

From (4) to (6), it is found that the *LCL* filter can provide the ripple attenuation of -60 dB/decade while the *L* filter has the attenuation of only -20 dB/decade [11]. To avoid the resonance issue, which can cause the system to become unreliable, the *LCL* filter components are chosen using the design process as explained in [10], [11]. The L_1 is calculated by using the ripple factor of the switching frequency component to the rated current. The C_f is limited by the reactive power absorption. The L_2 is determined by considering the attenuation ratio.

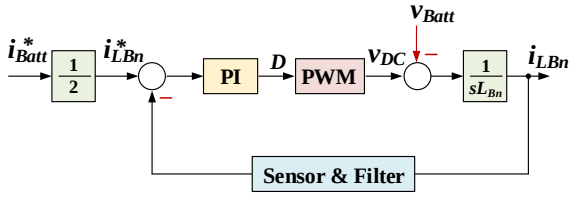

(a) Current loop controller

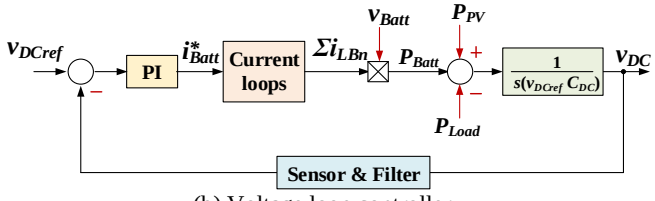

(b) Voltage loop controller

Fig. 10. The Interleave bidirectional DC-DC converter with current-voltage loop controllers.

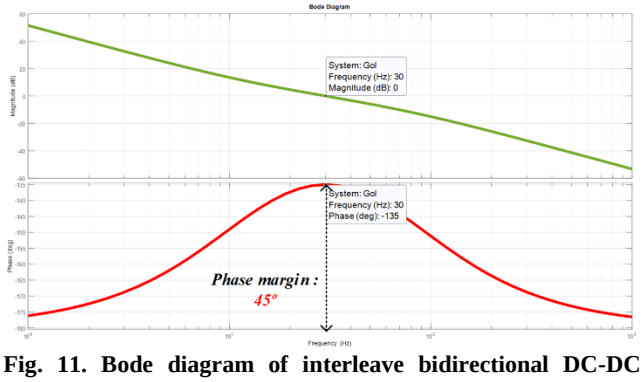

Fig. 11. Bode diagram of interleave bidirectional DC-DC converter control system.

3. EXPERIMENTAL SETUP AND CASE STUDY

The hardware prototype of the off-grid single-phase hybrid inverter is implemented, as illustrated in Fig. 9. Table 1, summarizes the key data of the proposed hybrid inverter. Table 2, displays the designed parameters of a 5-kW full-bridge DC-AC inverter with an MPPT boost DC-DC converter and an *LCL* filter. Besides, a 3-kW interleaved bidirectional DC-DC converter is employed coupled with a 300 V battery. Two real-time control units are developed on TMS320F28379D 32-bit microcontrollers which one for controlling DC-AC inverter and boost DC-DC converter, and the other for controlling the interleaved bidirectional DC-DC converter.

Table 1. Off-grid Hybrid Inverter Technical Data

Parameters	Value
AC nominal voltage (rms)	220 Vac
AC nominal frequency	50 Hz
AC maximum current (rms)	23 A
AC maximum power	5 kW
Nominal DC link, v_{DC}	400 Vdc
PV input voltage, v_{PV}	130 – 600 Vdc
Battery voltage, v_{batt}	300 Vdc
PWM technique	Hybrid
Switching frequency for	
- Full-bridge DC-AC inverter	20 kHz
- PV Boost DC-DC converter	20 kHz
- Bidirectional DC-DC converter	20 kHz

Table 2. Parameters of Hybrid Inverter's Power Stages

Parameters	Value
Boost inductor, L_{BT}	2 mH
Boost filter capacitor, C_{BT}	75 µF
Inverter side inductor, L_1	0.8 mH
Grid side inductor, L_2	0.4 mH
DC bus capacitor, C_{DC}	1,200 µF
Bidirectional inductor, L_{B1} and L_{B2}	1 mH
Bidirectional filter capacitor, C_{Batt}	195 µF
IGBTs	650 V, 80 A
Diodes	600 V, 60 A

The PI controllers for voltage and current controllers of interleaved bidirectional DC-DC converter are considered by applying an extended symmetrical optimization method, as proposed in [22],[23]. This method recommends that, to have an acceptable overshoot, the PI controller's phase margin should be in the range of 30° - 65° to assure the stability of the control system. From the closed loop control diagrams in Fig. 10, the parameters of PI controllers are

designed based on switching frequency of 20 kHz and the bandwidth is 30 Hz. Table 3, shows the parameters used in voltage and current control loops. Fig. 11 depicts the Bode diagram of the interleaved bidirectional DC-DC converter control system. It is discovered that the phase margin is 45° which can achieve the recommended value. Additionally, Section 4 presents of the reactions in the time domain.

Table 3. Parameters of Close-loop Controllers

Parameters	Value
Current loop: Proportional gain, K_i	0.2667
Current loop: Integral time, T_i	0.65 ms
Voltage loop: Proportional gain, K_v	0.7685
Voltage loop: Integral time,, T_v	5.1 ms
PWM delay time, T_d	40 µs
Current loop: Equivalent delay time, T_{di}	0.85 ms
Sensor & Filter delay time, T_f	0.2 ms

Table 4. List of Experimental Test

Time	Detail
0-20 s	PV = 0 kW, Load = 1 kW
20-35 s	PV ramps up to 3 kW, Load = 1 kW
35-65 s	PV = 3 kW, Load steps up to 2 kW
65-80 s	PV ramps down to 0 kW, Load = 2 kW
80-100 s	PV = 0 kW, Load = 2 kW

The test system is similar to Fig. 1 which consist of single-phase hybrid PV-battery system connects with AC linear and non-linear loads via the line impedance of 0.24 + *j*0.15 Ohm. As well, the experimental setup consists of the PV simulator, the Battery simulator, and the RLC simulator, which represent PV systems, energy storage systems (the HV lithium-ion 300V), and a linear load, respectively. The diode-bridge rectifier with resistance loads is chosen to represent the non-linear load.

The off-grid operation is explored using fluctuations in PV power generation and load demand for power to investigate the control capabilities of the proposed hybrid inverter. The variations of PV power are created by adjusting the values of i_{LBref} of boost DC-DC converter in Fig. 4. At initial, the PV is unavailable and the load demand is 1 kW at power factor of 0.95. After that, the PV ramps the power up to 3 kW and the load is stepped up to 2 kW with a 0.95 power factor. The detail of experimental examination is described in Table 4.

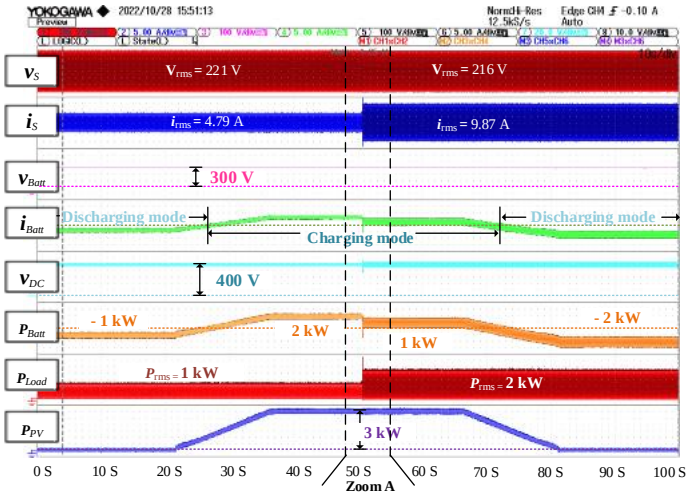

(a) The main results of the hybrid inverter

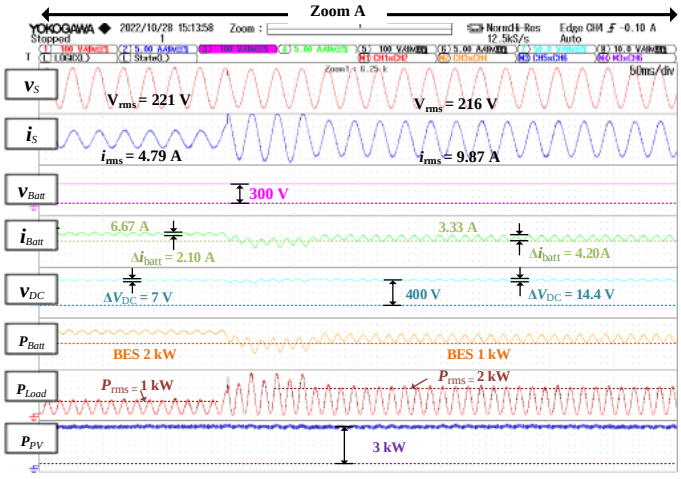

(b) The changes between 45 s and 55 s (Zoom A)

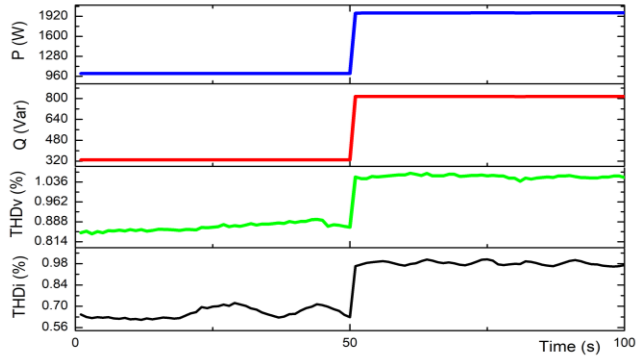

(c) *P* and *Q* (*rms* values) and harmonic distortions

Fig. 12. Experimental results in Case 1) Non-harmonic load

The growth of domestic non-linear loads, such as smart devices, inverter-based electric appliances, and LED lightings, can raise the level of harmonic distortions in the isolated electrical system. The proposed hybrid inverter should perform well even in environments with very high

harmonic pollution. Therefore, this hybrid inverter is tested under two different load types, as follows:

Case 1) Non-harmonic load.

Case 2) Harmonic load which is a mix of linear and non-linear loads.

The goal of this experiment is to verify the off-grid hybrid inverter operation in a range of situations that can occur in an actual isolated system. In a hybrid PV-battery system, the power balancing mechanism should be provided for controlling the DC link voltage via the interleaved bidirectional DC-DC converter. Rapid charging and discharging are essential for the effective management of the isolated system. Moreover, the full-bridge DC-AC inverter can function properly even when a highly non-linear load is connected.

4. EXPERIMENTAL RESULTS

The waveform outputs are measured by high bandwidth oscilloscope with 8 channels (YOKOGAWA model DLM4000). The harmonic distortions, *RMS* values of active and reactive powers are recorded by the digital power meter (YOKOGAWA model WT333E) with the sampling time of 1 second.

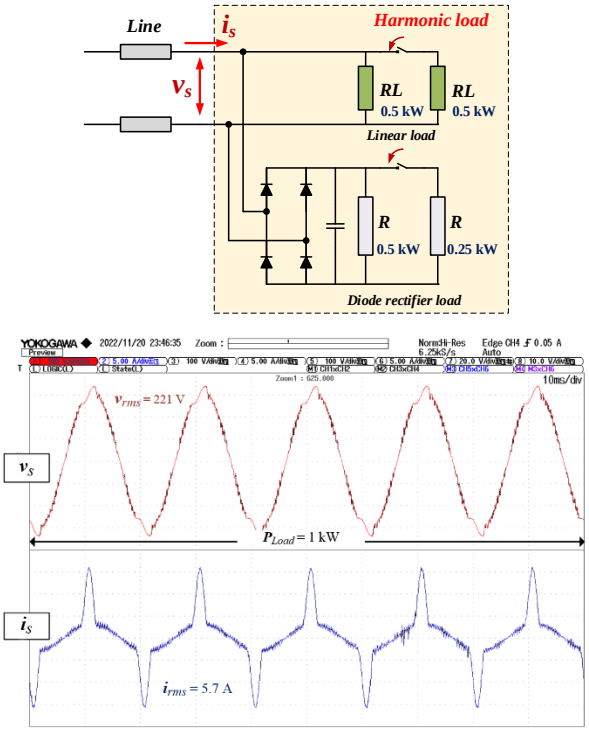

Fig. 13. Harmonic load and its waveforms

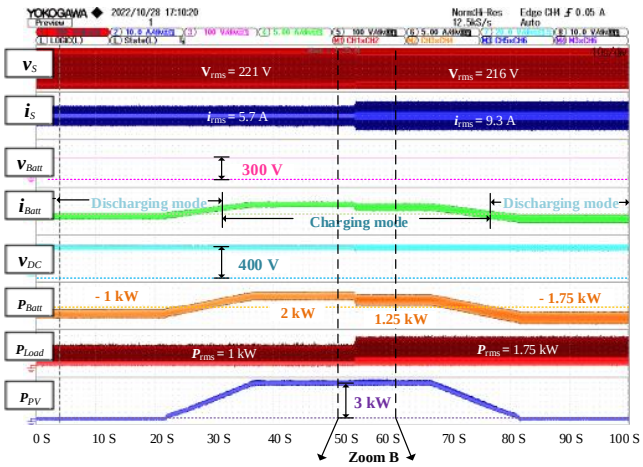

(a) The main results of the hybrid inverter

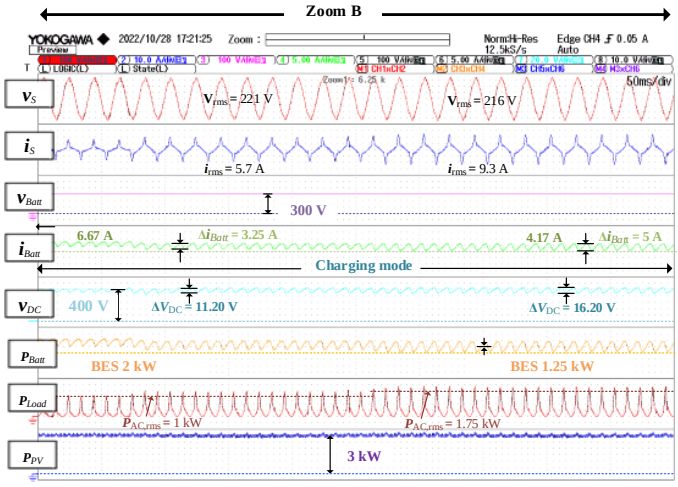

(b) The changes between 48 s and 60 s (Zoom B)

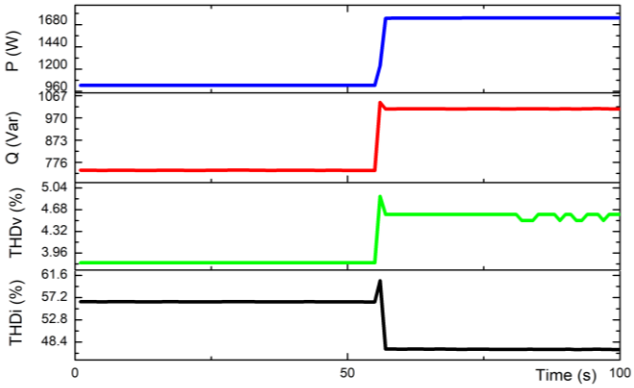

(c) *P* and *Q* (*rms* values) and harmonic distortions

Fig. 14. Experimental results in Case 2) Harmonic load.

Case 1) Non-harmonic load

Fig. 12 (a) shows the main test results which include: AC output voltage and current (v_S and i_S), battery current, voltage and power (v_{Batt}, i_{Batt} and P_{Batt}), DC bus voltage (v_{DC}), PV power (P_{PV}) and load demand (P_{Load}). The experimental results demonstrate that the proposed off-grid hybrid inverter can handle rapid variations in PV generation

and load consumption while maintaining low switching and battery current ripples. The control performance in each section is explained below.

During the time interval 0-20s: There is no PV generation at first. As a result, the battery is the only energy source capable of supporting the AC load at 1 kW and 0.33 kVar (power factor of 0.95). To discharge power from the HV battery, the bidirectional DC-DC converter works in the boost mode.

During the time interval 20-35s: There is a load requirement of 1 kW, but the PV power grows from 0 to 3 kW. The HV battery is charged when the PV power is in excess of the load requirement, and the bidirectional DC-DC converter switches to buck mode, absorbing the excess power (typically approximately 2 kW).

During the time interval 35-65s: The power demand from the load unexpectedly stepped from 1 kW to 2 kW, while the PV power remained exactly the same at 3 kW. Additionally, the reactive power is also changed to 0.82 kVar to maintain the power factor of 0.95 (see Fig. 12 (c)). However, the charging power is gradually reduced from 2 kW to 1 kW while the bidirectional DC-DC converter continues to operate in the buck mode. As shown in Fig. 12 (b), it is found that the battery current is changed from 6.67 A to 3.33 A within 3 ms while the voltage at the DC link momentarily falls before before recovering to the reference value of 400 V.

During the time interval 65-80s: The PV power steadily decreases from 3 kW to 0 kW, while the load demand remains constant at 2 kW. When the PV energy drops below 2 kW, the bidirectional DC-DC converter changes to the boost mode to discharge extra power in conjunction with the PV power to supply the AC load.

During the time interval 80-100s: The load requirement is 2 kW, but the PV power is 0 kW. Hence, the HV battery is the only available supply capable of satisfying the load requirements. The bidirectional DC-DC converter remains in boost mode to supply 2 kW to the AC load.

It is found that using hybrid PWM with the *LCL* filter allows the DC-AC inverter to generate AC output signals with very low switching ripples throughout the test. The AC output current and voltage waveforms, as illustrated in Fig. 12 (b), are nearly pure sinusoidal. Fig. 12 (c) shows that the total harmonic distortion of output current, THDi, is less than 1 %, and the total harmonic distortion of output voltage, THDv, is less than 1.2 %.

At the DC side, because of the interleaved topology, the DC link voltage ripple (peak to peak, Δv_{DC}) ranges from 7 V to 14 V, and the battery current ripple (peak to peak, Δi_{Batt}) ranges from 2.1 A to 4.2 A.

Case 2) Harmonic load

At initial, the 1 kW harmonic load is made up of a 0.5 kW *RL* load and a bridge diode rectifier with 0.5 kW resistive load. The voltage and current waveform of this 1 kW harmonic load is shown in Fig. 13. The harmonic distortions of output voltage and current are demonstrated in Table. 5 which mostly are 3rd, 5th and 7th harmonic orders. The THDi and THDv are 56.8 % and 3.8 %, respectively. The load stepping up is achieved by increasing linear load to 1 kW and non-linear load to 0.75 kW. Besides, the reactive power is increased from 0.74 kVar to 1 kVar, which causes the power factor to increase from 0.81 to 0.87.

Table 5. Harmonic Distortions of Non-Linear Load

Order	%HDv		%HDi	
	1 kW	1.75 kW	1 kW	1.75 kW
3	1.30	1.29	41.04	41.04
5	2.32	2.32	31.47	31.49
7	2.33	2.33	20.03	20.06
9	1.16	1.16	9.54	9.56
11	0.60	0.60	3.14	3.15
13	0.14	0.14	0.56	0.56
15	0.19	0.18	0.63	0.63

Similar to the case 1, Fig. 14 (a) illustrates that the proposed hybrid inverter can perform the power balancing among fast variations of PV power and load demand, even though the level of harmonic distortion in the isolated system is dramatically increased. Furthermore, the ripples of DC voltage and battery current are significantly higher than in the non-harmonic load case, as can be seen in Fig. 14 (b). It is found that the Δv_{DC} ranges from 11.2 V to 16.2 V, and the battery current ripple (peak to peak, Δi_{Batt}) ranges from 3.25 A to 5 A.

As shown in Fig. 14 (c), the addition of the non-linear load causes an obvious increase in THDi and THDv of AC output voltage and current over the duration of the test, which THDi is in between 46 % and 57 % and THDv is in the range of 3.8 % to 4.6 %. Then, the concern of power loss causing by the raise of ripples and harmonic distortions becomes more serious, and a larger size of filter capacitor and passive filter may be considered.

5. CONCLUSION

The experimental testing verifies that the proposed off-grid single-phase hybrid PV – HV battery inverter with a two-stage interleaved bidirectional DC-DC converter can deal with rapid changes in PV output and load demand in an isolated system, both low and high harmonic distortion conditions. The interleaved bidirectional DC-DC converter can handle the power balancing mechanism by controlling the HV battery charging/discharging current with a fast response. The two-phase interleaved topology also provides a low battery current ripple, improving power conversion efficiency. However, increasing the harmonic load intends

to exacerbate the ripples of DC bus voltage and battery current, which can reduce the battery's service life. Moreover, the DC-AC inverter with *LCL* filter and Hybrid PWM control technique facilitates output ripples and leakage current, making the AC output waveform close to the pure sinusoidal.

ACKNOWLEDGMENT

This work is in "Interleaved Bi-directional Converter for Hybrid inverter with PV and battery system" project (number R2566E006) supported by Centre of Excellence on Energy Technology and Environment (CeTe) and Faculty of Engineering, Naresuan University, Thailand.

REFERENCES

[1] Rana, M. M.; Uddin, M.; Sarkar, M.R.; Shafiullah, G.M.; Mo, H. and Atef, M. 2022. A review on hybrid photovoltaic – Battery energy storage system: Current status, challenges, and future directions. In *Journal of Energy Storage*, Vol. 51, 2022, doi: 10.1016/j.est.2022.104597.

[2] Market Resource Future (2022). Hybrid Battery Energy Storage System Market Projected to Hit USD 22.3 Billion at a 7.20% CAGR by 2030. *GlobeNewswire*." Retrieved November 20, 2022 from the World Wide Web: https://www.globenewswire.com/news-release/2022/09/27/2523228/0/en/Hybrid-Battery-Energy-Storage-System-Market-Projected-to-Hit-USD-22-3-Billion-at-a-7-20-CAGR-by-2030-Report-by-Market-Research-Future-MRFR.html

[3] Subramaniam, U.; Vavilapalli, S.; Padmanaban, S.; Blaabjerg, F.; Holm-Nielsen, J.B. and Almakhles, D. A. 2020. Hybrid PV-Battery System for ON-Grid and OFF-Grid Applications—Controller-In-Loop Simulation Validation. In *Energies* 2020, 13, 755. https://doi.org/10.3390/en13030755

[4] Junhuathon, N., & Marungsri, B. (2019). Planning for battery energy storage systems control to enhance stability of the microgrid using power forecasting. *GMSARN International Journal*, *13*, 45-51.

[5] Svarc, J. (2020). Solar Battery System Types – AC vs. DC Coupled. *Clean Energy Reviews*. Retrieved November 20, 2022 from the World Wide Web: https://www.cleanenergyreviews.info/blog/ac-coupling-vs-dc-coupling-solar-battery-storage

[6] Mexis, I. and Todeschini, G. 2020. Battery Energy Storage Systems in the United Kingdom: A Review of Current State-of-the-Art and Future Applications. In *Energies*. 2020; 13(14):3616, doi: 10.3390/en13143616.

[7] Zhang, J.; Lai, J. -S.; Kim, R. -Y. and Yu, W. 2007. High-Power Density Design of a Soft-Switching High-Power Bidirectional dc–dc Converter. In *IEEE Transactions on Power Electronics*, vol. 22, no. 4, pp. 1145-1153, July 2007, doi: 10.1109/TPEL.2007.900462.

[8] Namboodiri, A. and Wani, H.S. 2014. Unipolar and Bipolar PWM Inverter. In *IJIRST –International Journal for Innovative Research in Science & Technology*, Issue 7. 2014.

[9] Kot, R.; Stynski, S.; Stepien, K.; Zaleski, J. and Malinowski, M. 2016. Simple Technique Reducing Leakage Current for H-Bridge Converter in Transformerless Photovoltaic Generation. In *Journal of Power Electronics*, vol. 16, p. 10, 01/20 2016, doi: 10.6113/JPE.2016.16.1.153.

[10] Jo, J.; Liu, Z. and Cha, H. 2019. A New Design Method of LCL Filter for Single Phase Grid Connected Power Converter. In *2019 International Symposium on Electrical and Electronics Engineering (ISEE)*, 2019, pp. 189-193, doi: 10.1109/ISEE2.2019.8921036.

[11] Ali, A.; Shanmugham, P. and Somkun, S. 2017. Single-phase grid-connected voltage source converter for LCL filter with grid-current feedback. In *2017 International Electrical Engineering Congress (iEECON)*, 2017, pp. 1-6, doi: 10.1109/IEECON.2017.8075720.

[12] Al-Obaidi, N. A.; Abbas, R. A. and Khazaal, H.F. 2022. A Review of Non-Isolated Bidirectional DC-DC Converters for Hybrid Energy Storage System In *2022 5th International Conference on Engineering Technology and its Applications (IICETA)*, 2022, pp. 248-253, doi: 10.1109/IICETA54559.2022.9888704.

[13] Vo Thanh, V., Vinh, N., & Van Dai, L. (2022). Partly-Isolated DC-DC Converter for DC Bus Battery- PV Solar Energy System. *GMASARN International Journal*, *16*, 263-272.

[14] Yang, Y.; Ma, J.; Ho, C. N. -M. and Zou, Y. 2015. A New Coupled-Inductor Structure for Interleaving Bidirectional DC-DC Converters. In *IEEE Journal of Emerging and Selected Topics in Power Electronics*, vol. 3, no. 3, pp. 841-849, Sept. 2015, doi: 10.1109/JESTPE.2015.2443178.

[15] Yu, W.; Qian, H. and Lai, J. -S. 2008. Design of high-efficiency bidirectional DC-DC converter and high-precision efficiency measurement. In *2008 34th Annual Conference of IEEE Industrial Electronics*, 2008, pp. 685-690, doi: 10.1109/IECON.2008.4758036.

[16] Omara, A. M. and Sleptsov, M. 2016. Bidirectional interleaved DC/DC converter for electric vehicle application. In *2016 11th International Forum on Strategic Technology (IFOST)*, 2016, pp. 100-104, doi: 10.1109/IFOST.2016.7884201.

[17] Babaa, S. E.; El Murr, G.; Mohamed, F. and Pamuri, S. 2018. Overview of Boost Converters for Photovoltaic Systems. In *Journal of Power and Energy Engineering*, Vol.6 No.4, 2018, doi: 0.4236/jpee.2018.64002.

[18] Boonraksa, P., Boonraksa, T., and Marungsri, B. (2022). Enhancement of the Maximum Power Point Tracking for the Solar Power Generation using ZETA Converter Circuit. *GMSARN International Journal*, *13*, 273-278.

[19] Tofoli, F. L.; de Castro Pereira, D. and de Paula, W. J. 2015. Comparative Study of Maximum Power Point Tracking Techniques for Photovoltaic Systems. In *International Journal of Photoenergy*, vol. 2015, p. 812582, 2015/02/04, doi: 10.1155/2015/812582.

[20] Zhu, Y.; Wen, H.; Chu, G.; Hu, Y.; Li, X. and Ma, J. 2021. High-Performance Photovoltaic Constant Power Generation Control with Rapid Maximum Power Point Estimation. In *IEEE Transactions on Industry Applications*, vol. 57, pp. 714-729, Jan.-Feb. 2021, doi: 10.1109/TIA.2020.3029128.

[21] SMA Solar Technology AG. Leading Leakage Current. (Leakage current-TI-en-26). Technical Information on the design of SMA's transformerless inverters.

[22] Somkun, S.; Sirisamphanwong, C. and Sukchai, S. 2015. A DSP-based interleaved boost DC–DC converter for fuel cell

applications. In *International Journal of Hydrogen Energy*, vol. 40, pp. 6391-6404, 04/01 2015, doi: 10.1016/j.ijhydene. 2015.03.069.
[23] Preitl, S. and Precup, R.-E. 1999. An extension of tuning relations after symmetrical optimum method for PI and PID controllers. In *Automatica*, vol. 35, no. 10, pp. 1731-1736, doi: 10.1016/S0005-1098(99)00091-6.